

## DISEASE-INDUCED ALTERATIONS IN THE REFLECTANCE SPECTRUM OF GRAPE LEAVES

Pâmela PITHAN<sup>1</sup>, Lucas GARRIDO<sup>3</sup>, Diniz ARRUDA<sup>1</sup>, Adriane THUM<sup>1,2</sup>, Rosemary HOFF<sup>3</sup>,  
Jorge DUCATI<sup>1\*</sup>

<sup>1</sup>Universidade Federal do Rio Grande do Sul, Av. Bento Gonçalves 9500, 91501-970 Porto Alegre, Brazil

<sup>2</sup>Universidade do Vale do Rio dos Sinos, Av. Unisinos 950, 93020-190 São Leopoldo, Brazil

<sup>3</sup>Empresa Brasileira de Pesquisa Agropecuária, R. Livramento 515, 95701-008 Bento Gonçalves, Brazil

\*Corresponding author:[ducati@if.ufrgs.br](mailto:ducati@if.ufrgs.br)

### Abstract:

**Context and purpose of the study** - Phytopathogenic diseases impact the development and yield of grapevines, resulting in economical, social and environmental losses. Sick plants have their metabolism changed, leading to alterations in their reflectance spectra. Little is known on these alterations, and a better knowledge could be used in the development of sensors able to detect diseases through fast, non-destructive techniques. The present study was aimed at detecting spectral changes on the reflectance spectra of vines of cv. Cabernet Sauvignon, with early symptoms of downy mildew, powdery mildew, black-foot and Petri disease, describing the spectral domains where alterations are measurable with respect to healthy control vines. This information can be used to the development of low-cost devices which can perform real-time field measurements to early assessment of vineyard health status.

**Material and methods** - Plants of Cabernet Sauvignon grown in pots and kept in a greenhouse were inoculated with the pathogens causing mildew, powdery mildew, black-foot and Petri disease. In early stages of disease development, reflectance measurements were performed using a FieldSpec 3 spectroradiometer, which were compared with data from healthy plants. The investigation began with discriminant analysis, which revealed that symptomatic plants are indeed separated from the control ones. Reflectance spectra were therefore further investigated and alterations on the shape of the spectra, characteristic of each disease, were looked for. The disease descriptors were based on ratios between spectral features internal to a spectrum, a procedure which allowed the derivation of parameters intrinsic to each disease.

**Results** - A set of thresholds, which are the intensity ratios of reflectance at selected wavelengths, was derived for the studied diseases. The selected wavelength ratios were 443/496, 443/573, 443/695, 443/1900, 496/573, 496/695, 516/1900, and 1900/2435 (values in nanometers), for which the spectra from symptomatic plants present shape changes of as much as 20% in reflectance with respect to healthy plants. The observed spectral deformations are larger for black-foot and powdery mildew, but some wavelength ratios are also indicators of downy mildew and Petri disease. Data from near-infrared are in general more useful, compared with measurements at 1900 and 2435nm.

**Keywords:** Grapevine diseases, leaf reflectance, spectroradiometry, disease detection.

### **1. Introduction**

Biotic diseases induce noticeable alterations on the reflectance spectrum of plants, especially due to changes on chlorophyll and water content, between other factors. Naidu et al. (2009) reported the differences in leaf reflectance measurements at specific wavelength intervals between leafroll-virus infected leaves of grapevines. Graeff et al. (2006) in a study carried out with wheat plants indicated that disease detection and discrimination of powdery mildew by means of reflectance measurements may be realized by the use of specific wavelength ranges. Methods based in visible and near-infrared spectroscopy have been proposed, as in Junges et al. (2018) who reported effects on the spectra of grapevines infected by leaf-roll virus, observed mainly in visible light and at near infrared. However, detailed descriptions of which spectral changes occur and applications of this knowledge which can benefit productive processes have yet to be reported. In fact, usually the detection of a disease in a crop happens when the disease has already attained

a relatively large part of the field, a condition which makes protective measures hard to apply. Early detection can make possible preventive actions, reducing losses and costs, carrying possible environmental benefits through reduction of pesticides (Mahlein, 2016; Komárek et al., 2010). Fast, real-time, low-cost and non-destructive techniques can be advantageous.

For this research, we selected four diseases, two that attack all green parts of the vine (downy mildew, *Plasmopara viticola*, and powdery mildew, *Uncinula necator*) and two that attack trunks and roots, the Petri disease which can be caused by *Phaeoacremonium* spp. and the black-foot disease, *Dactylonectria macrodidyma*. Here, we report results from the use of spectroradiometry on disease and healthy plants of *Vitis vinifera*, var. Cabernet Sauvignon, observed *in vivo*, in a greenhouse.

## **2. Material and methods**

*Plant materials* - Samples of healthy and infected plants of *Vitis vinifera*, var. Cabernet Sauvignon were prepared at the Phytopathology Laboratory of the Embrapa Grape & Wine, an unit of Brazilian Agricultural Research Corporation (EMBRAPA) located in Bento Gonçalves, Rio Grande do Sul State, Brazil, where a collection of filamentous fungus is available. Seventy Cabernet Sauvignon plants were produced from vine cuttings, which developed new roots.

Isolated pathogens of *Dactylonectria macrodidyma*, and of *Phaeoacremonium* spp. were replicated to PDA (potato-dextrose-agar) growth medium, maintained at 24°C and photoperiod of 12 hours, during 20 days. Ten plants for each pathogen were prepared. For these two diseases unique batches of ten control plants were prepared. We allowed a period of thirteen days between inoculation and spectral measurements.

Inocula of *Plasmopara viticola* were obtained by collecting infected leaves from a Cabernet Sauvignon vineyard in the region. This batch of ten plants, along with a batch of ten control plants, was incubated at 24°C and relative humidity of 92%, during eight days with a photoperiod of 12 hours.

*Uncinula necator* inoculum occurred spontaneously on leaves Cabernet Sauvignon variety vine plants inside the greenhouse. Ten plants were prepared, and in this case ten control plants were sprayed with a fungicide of the triazol group to avoid infection by the pathogen.

Finally, we had batches of ten infected plants for each of four pathogens, and three batches of ten control plants each, being ten control plants for downy mildew, ten control plants for powdery mildew, and ten control plants for diseases attacking the vine root system.

The procedures described above were done for the 2017 campaign. This was repeated with new plants for a second campaign in 2018, with the difference that for downy mildew we had only five control plants.

*Plant measurements* - Spectroscopic measurements used a FieldSpec 3 spectroradiometer with spectral sensitivity between 350nm and 2500nm. A typical spectrum provides reflectance values between 0.0 and 1.0 at intervals of one nanometer. Measurements used the ProbeLeaf Clip, with an internal halogen light source and also an internal reference plate of Spectralon® used for calibration.

The observational procedure was as follows: for each plant three leaves were selected at mid-height, marked and measured at their adaxial side, avoiding nerve ribs. An *in vivo* leaf full measurement was made of four consecutive readings. A full batch of asymptomatic plants was measured, then the batch of symptomatic plants. All spectra were normalized to allow for direct operations between them.

## **3. Results and discussion**

In Figure 1 we present typical spectra of symptomatic and control plants. Spectral alteration in plants, and in our case, grapevines, can be subtle and appropriate methods to detect these alterations must be developed. However, detection of such subtle features is possible when the analyzed spectra have a high signal-to-noise (SNR) ratio. In our case, typical SNR values were 5900 at  $\lambda = 850\text{nm}$  and 7500 at  $\lambda = 1800\text{nm}$ , indicating high-quality measurements (Schroeder, 1999), allowing us to perform operations involving spectra of control and symptomatic leaves, in the form given by Eq. 1:

$$\text{Spectrum ratio} = \frac{\text{Control}_n}{\text{Disease}_n} \quad (1)$$

In Eq. 1, a "spectrum ratio" is the result of the division, at each wavelength, of the reflectance value of a control plant by the reflectance value of a symptomatic plant. Given that spectral alterations, as already noted, are subtle, both spectra are almost equal, and the resulting quotient tends to display values nearly

equal to unity along the entire wavelength domain. However, if differences exist, and are consistently present in several spectrum-ratios derived from different pairs of spectra, it would be possible that the wavelengths where these persistent differences arise are effectively regions of the vine spectra where metabolic effects of a disease on a plant lead to spectral alterations; in these regions, a non-unity quotient will exist. An analysis of the wavelengths with consistent non-unity quotients revealed the spectral regions where diseases provoked spectral alterations. Some typical spectrum ratios are presented in Figure 2.

A preliminary analysis of these wavelengths produced an additional perception. It was perceived that spectral alterations due to different diseases left their marks in nearly the same wavelengths: for example, downy mildew and black-foot alter a normal spectrum at the same places. However, the metabolic changes induced on the plant by each disease are characteristic, and this leads to spectral alterations which have magnitudes typical of each disease. The final perception, thus, is that a spectrum of a symptomatic plant, with respect to a spectrum of a control plant, presents not only spectral alterations in certain wavelengths, but also the magnitudes of these alterations are characteristic of each disease. The shape of the spectrum for a certain disease is unique, and a possible way to describe this shape is using descriptors internal to a spectrum, that is, descriptors which are ratios between reflectance values at the characteristic wavelengths. In this way, it is possible to make a set of ratios which are characteristic of each disease. A set of ratios derived in this way has the advantage of being internal of a spectrum, that is, the information revealing the disease is fully contained inside the spectrum of a symptomatic plant. The advantage of this method is that it could be possible to reach a diagnosis by measuring reflectance at certain wavelengths.

When we analyzed our database using data from the second year of observations, it was perceived that there were an association between the control plants and the corresponding batch of symptomatic vines. This comes from the fact that both groups had their start from the same conditions; for another pair control-disease, involving another disease, the starting conditions were different. The conclusion was that not only we have to consider the internal descriptors of a symptomatic plant to obtain a diagnosis, but even then, a calibration measurement of a healthy plant has to be associated.

From Figure 2 it was seen that certain wavelengths are indicators of disease effects. These wavelengths are, in the visible, at 443, 496, 516, 573 and 695nm, and at the mean infrared, at 1420, 1900 and 2435nm. All diseases present spectral alterations in these wavelengths, but with varying intensities, because each pathogen behaves in a characteristic way at each wavelength. Ratios between reflectance at these wavelengths showed better performances to differentiate between diseases for the 443/496, 443/573, 443/695, 443/1900, 496/573, 496/695, 516/1900, and 1900/2435 combinations.

Data from control plants were used for each season (2017 and 2018), and Table 1 shows how the thresholds behave for the studied diseases derived for each year, calibrated by the respective control measurements.

Table 1 expresses how much the spectrum of a symptomatic plant is deformed with respect to the spectrum of a healthy plant. Beginning with the deformations expressed by the 443/496 ratio, we see that black-foot disease leads to a deformation of about 10%. This same disease, black-foot, also deforms the spectrum for the 443/573 ratio but at a larger scale (up to 17%); for this ratio a systematic spectral deformation is also observed for powdery mildew, but at a smaller scale (3 to 5%). These two diseases are also observed for the 443/695 ratio, at scales up to about 20% (black-foot) and 5 to 8% (powdery mildew).

For downy mildew, the 443/1900 ratio could be a useful indicator, since spectral deformations of up to 14% were observed. The ratios 496/573, 496/695 and 510/1900 are useful indicators of black-foot and powdery mildew symptoms. The ratio 1900/2435 seems to be, from our data, less useful.

Further examination of Table 6 shows that, in some cases, the spectral deformation is large, but changes direction from a season to the next. This happens for Petri disease in 443/1900 and also for powdery mildew in this same ratio. The same is for Petri in 496/695 and in 516/1900 for downy mildew. The method, therefore, works better for detection of black-foot and powdery mildew. In certain cases it can be appropriate for downy mildew and Petri disease, where a spectral deformation of the sick plant is observed, even if the deformation direction changes for year to year.

#### **4. Conclusions**

The method presented here produces real-time data that can be automatically processed to give a diagnosis on the plant health status. This can be done by associating to the measuring device a processor capable of performing the basic operations involving the observed spectra. The observing device does not need to have

the capability of fully observing a spectrum in high resolution (which would be a spectro-radiometer); given that only some pre-determined wavelengths are needed, a simpler, less-expensive photo-sensitive device can be projected to perform the programmed tasks, properly tuned to the diseases to be detected.

### 5. Acknowledgments

This study was carried out with the support of the Coordination of Improvement of Higher Level Personnel (CAPES- Brazil) - Financing Code 001.

### 6. Literature cited

- GRAEFF, S., LINK, J., CLAUPEIN, W. 2006. Identification of powdery mildew (*Erysiphe graminis* sp. *tritici*) and take-all disease (*Gaeumannomyces graminis* sp. *tritici*) in wheat (*Triticum estivum* L.) by means of leaf reflectance measurements. Central European Journal of Biology 1, 275-288.
- JUNGES, A.H., DUCATI, J.R., LAMPUGNANI, C.S., ALMANÇA, M.A.K. 2018. Detection of grapevine leaf stripe disease symptoms by hyperspectral sensor. Phytopathologia Mediterranea 57, 399-406.
- KOMÁREK M., ČADKOVÁ E., CHRASTNÝ V., BORDAS F., BOLLINGER J-C. 2010. Contamination of vineyard soils with fungicides: A review of environmental and toxicological aspects. Environment International 36, 138-151.
- MAHLEIN A.-K. 2016. Plant disease detection by imaging sensors – Parallels and specific demands for precision agriculture and plant phenotyping. Plant Disease, 100 (2), 241-251.
- NAIDU, R. A., PERRY, E. M., PIERCE, F. J., MEKURIA, T. 2009. The potential of spectral reflectance technique for the detection of grapevine leafroll-associated virus in two red-berried wine grape cultivars", Computers and Electronics in Agriculture, v. 66, p. 38-45.
- SCHROEDER, D. J. 1999. Astronomical Optics. Cambridge: Academic Press.

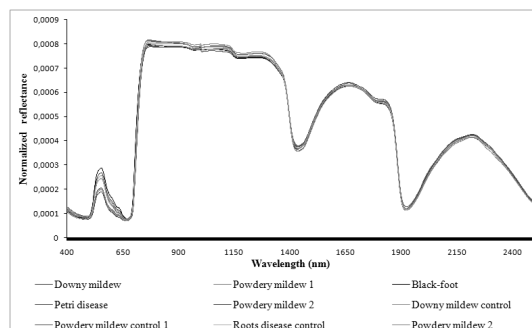


Figure 1: Typical reflectance spectra.

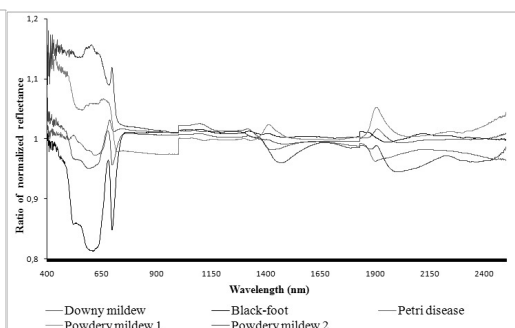


Figure 2: Divisions between spectra, control/sick.

Table 1: Thresholds for the studied diseases for each year (2017 and 2018).

	Downy mildew		Black-foot		Petri disease		Powdery mildew	
	2017	2018	2017	2018	2017	2018	2017	2018
443/496	0.98	1.00	0.94	0.86	0.99	0.96	1.05	0.99
443/573	0.94	1.06	0.83	0.81	0.97	1.01	0.92	0.97
443/695	0.92	1.04	0.83	0.82	0.98	1.05	0.91	0.96
443/1900	1.00	0.86	1.02	0.93	0.94	1.20	0.95	1.16
496/573	0.95	1.05	0.88	0.92	0.97	1.04	0.95	0.96
496/695	0.94	1.04	0.88	0.96	0.99	1.08	0.94	0.98
516/1900	1.06	0.74	1.18	1.03	0.95	1.06	1.01	1.09
1900/2435	0.98	1.03	1.00	1.02	1.00	0.99	0.98	1.01